Obstacle Avoidance by DSmT for Mobile Robot in Unknown Environment

Huimin Chai[†]
School of Computer Science and Technology
Xidian University
Xi'an, China
chaihm@mail.xidian.edu.cn

Shaonan Lv
School of Computer Science and Technology
Xidian University
Xi'an, China

Min Fang
School of Computer Science and Technology
Xidian University
Xi'an, China

ABSTRACT

A method by Dezert-Smarandache theory (DSmT) is proposed for obstacle avoidance of mobile robot in unknown environment. The grid environment map is constructed for robot. On the basis of DSmT, the generalized basic belief assignment (gbba) is defined to evaluate the grid state: empty, has obstacle, and unknown. Then the belief values of the grid state from different time slice are combined by DSmT. Experiments including eleven typical simulation scenes are given. In these experiments, one scene test fails and the rest of ten scenes are successful in which robot can avoid all obstacles. The results show that the method is effective and available for mobile robot's obstacle avoidance in unknown environment.

CCS CONCEPTS

• Computing methodologies~Artificial life

KEYWORDS

Mobile robot, Obstacle avoidance, DSmT theory

1 Introduction

Obstacle avoidance is a key problem for mobile robot navigation in unknown environment. Robot can obtain information about unknown environment through their sensors, such as sonar, laser, visual and so on. Especially, sonar sensor is usually adopted as the main sensor of mobile robot owing to its low price and convenient applicability. On the basis of sensors data, robot perceives its surrounding to avoid obstacles. Therefore, the ability to deal with sensor data is very important for robot obstacle avoidance in unknown environment.

Recently, the main methods of obstacle avoidance for mobile robot are: artificial potential field [1,2], neural network[3,4], genetic algorithm[5,6], etc. However, artificial potential field method has drawbacks with local minima and the problem of goal nonreachable with obstacle nearby. Considering neural network and genetic algorithm, they have the problems of the great dependence on the method parameters and slow convergence rate.

Dempster-Shafer theory(DST, DS theory)[7] is a mainstream theory for data fusion and it can be used to model and fuse uncertain information. However, the DS theory cannot combine the highly conflicting evidences[8]. The Dezert-Smarandache theory is proposed by Dr. Jean Dezert in the year of 2002[9] and developed with Prof. Florentin Smarandache[10]. Compared with DS theory, the Dezert-Smarandache theory can construct the frame of discernment which is exhaustive but not necessarily exclusive. And it can deals with imprecise, uncertain or paradoxical data. Consequently, DSmT theory can be regarded as an extension of DS theory and has been employed in the research of mobile robot.

An evidence reasoning machine (ERM) based on DSmT theory is presented for mobile robot mapping in unknown dynamic environment [11]. Luige[12] presents an innovative algorithm for improvement of the walking robot dynamic stability using the DSmT theory. In the paper, the Dezert-Smarandache theory is used to fuse the sonar data to avoid obstacle.

The rest of the paper is organized as follows. In Section 2, the definitions in DSmT are introduced. In Section 3, the method of obstacle avoidance by DSmT is provided and the combination of sonar data from different time slice is described. The experiments follow in Section 4, before the concluding remarks of Section5.

2 DSmT Theory

DSmT theory is based on hyper-powerset (denoted as D^Ω) which is defined as the set of all composite propositions built from elements of Ω with the operators $\cup$ and $\cap$. Note that $\Omega = \{\theta_1, \theta_2, ...\theta_n\}$ is the frame of discernment which is a set of n complete propositions. The specific definition of hyper-powerset is as follows:

(1) $\emptyset, \theta_1, \theta_2, ..., \theta_n \in D^\Omega$

(2) If $A, B \in D^\Omega$, then $A \cap B \in D^\Omega$ and $A \cup B \in D^\Omega$

(3) No other elements belong to D^Ω, except propositions from (1) and (2).

On the basis of hyper-powerset, the generalized basic belief assignment(gbba) is defined:

CACRE '19, July 19–21, 2019, Shenzhen, China

ACM ISBN 978-1-4503-7186-5/19/07…$15.00
https://doi.org/10.1145/3351917.3351981

$$m(\varnothing) = 0, \sum_{A \in D^{\Omega}} m(A) = 1 \quad (1)$$

Under the same frame of discernment, suppose that there are two gbbas $m_1(\bullet)$ and $m_2(\bullet)$ which are from two different sources, respectively. The DSm classic(DSmC) rule of combination is provided[7]:

$$\forall C \in D^{\Omega}, m_{\mu^f}(\Omega)(C) \equiv m(C) = \sum_{X_1, X_2 \in D^{\Omega}, X_1 \cap X_2 = C} m_1(X_1) m_2(X_2) \quad (2)$$

For the DSmC rule of combination, no constraints can be added. However, there exists constraint in most practical applications of evidence fusion. Therefore, the DSm hybrid(DSmH) rule of combination is given :

$$m_{\mu}(\Omega)(C) \equiv \varnothing(C)[S_1(C) + S_2(C) + S_3(C)]$$

$$S_1(C) = \sum_{X_1, X_2 \in D^{\Omega}, X_1 \cap X_2 = C} m_1(X_1) m_2(X_2)$$

$$S_2(C) = \sum_{\substack{X_1, X_2 \in \varnothing \\ [(u(X_1) \cup u(X_2)) = C] \vee [(u(X_1) \cup u(X_2) \in \varnothing) \wedge (C = I_t)]}} m_1(X_1) m_2(X_2)$$

$$S_3(C) = \sum_{\substack{X_1, X_2 \in D^{\Omega} \\ (X_1 \cup X_2) = C \\ X_1 \cup X_2 \in \varnothing}} m_1(X_1) m_2(X_2) \quad (3)$$

where $\varnothing = \{\Phi, \varnothing_{\mu}\}$ is the constrain condition set that includes absolute empty condition Φ and relative empty condition $\varnothing_{\mu}$, and $I_t = \theta_1 \cup \theta_2 \cup ... \cup \theta_n$. $\varnothing(C)$ is nonempty characteristic function. If $C \in \varnothing$, the value of $\varnothing(C)$ is ‘0’, else is ‘1’.

3 Obstacle avoidance using DSmT

3.1 Model of sonar sensor

The measurement principle of sonar is: sonar send out cone-shaped wave to detect the objects. The wave will be reflected if it encounters an object. Thus, the distance from sonar to the object can be obtained. Since the detection range of sonar is a sector area, it is sure that the detected object is in the sector area, but not sure the exact position of the object. On the basis of the measurement principle, the detection range of sonar is further divided as shown in Fig. 1.

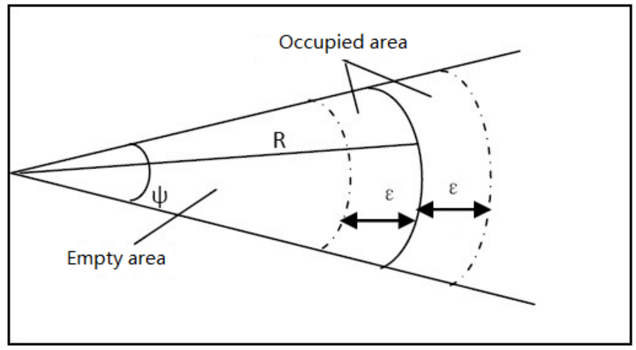

Figure 1 Measurement area division of sonar

R is the object distance measured by sonar, ε is the error of sonar reading, and ψ is the divergence angle of sonar. The measurement area of sonar is divided into two parts shown in Fig.1 :

- Empty area

It is located in the range of $[0, R-\varepsilon]$. In the empty area, the probability of exiting obstacle is zero.

- Occupied area

This area is in the range of $[R-\varepsilon, R+\varepsilon]$. In the occupied area, the probability of exiting obstacle is one.

In order to evaluate the position of obstacle, the grid environment map is constructed for robot. Three states of each grid on the map are defined as: empty, has obstacle, and unknown. For each grid, the state of empty represents that there is no obstacle. The state of has obstacle means that there exists obstacle in a grid. If the state of grid is unknown, it is not clear whether there is obstacle.

On the basis of the three states definition, the frame of discernment with DSmT theory is given: $\Omega = \{E, O\}$. In the discernment frame, E stands for the state of empty and O is for the state of has obstacle. The corresponding hyper-powerset is: $D^{\Omega}=\{\Phi, E, O, E \cup O, E \cap O\}$, which is based on the frame of discernment Ω. Φ denotes empty set, $E \cup O$ represents the grid state of unknown, and $E \cap O$ represents that part of grid is occupied by obstacle and the remaining is empty. Since $E \cap O$ can be regarded as the state of has obstacle, then constrain condition is added which is $\mu_f = (E \cap O \equiv \varnothing)$.

3.2 Function of gbba for grid state

For DSmT theory, a mapping $m(\bullet): D^{\Omega} \to [0,1]$ should be guaranteed which is the function of gbba. As shown in Fig.2, sonar is located at the origin O and x-axis is the central axis of sonar. OP1 is the distance measured by sonar. OP2 and OP3 respectively are: $OP2 = OP1 + \varepsilon$, $OP3 = OP1 - \varepsilon$, where ε denotes the error of sonar reading.

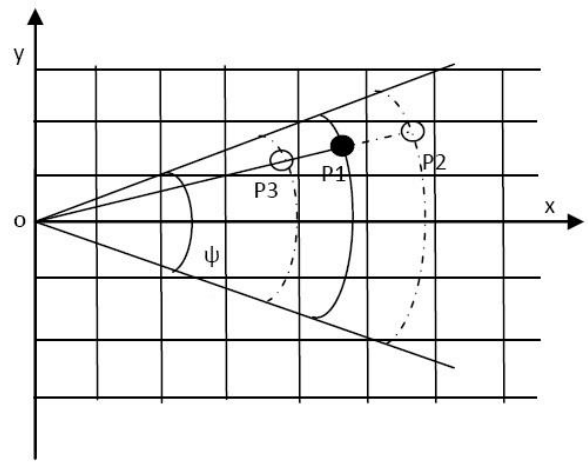

Figure 2 Computing model of belief assignment for state of grid

Let grid size be 80*80 in centimeters, and Suppose *d* denotes the real distance from the center of grid to sonar. The unit of distance is centimeter in this paper.

- If real distance d satisfied: $d < OP1 - \varepsilon$, it means that the grid falls in the empty area of sonar measurements. The function of gbba will be:

$$\begin{cases} m(O) = 0 \\ m(E) = 1 - d/(OP1 - \varepsilon)^2 \\ m(E \cup O) = 1 - m(E) \end{cases} \tag{4}$$

- If $OP1 - \varepsilon < d < OP1 + \varepsilon$, the grid falls in the occupied area of sonar measurement. Then there will be:

$$\begin{cases} m(O) = 1 - ((d\text{-}OP1)/\varepsilon)^2 \\ m(E) = 0 \\ m(E \cup O) = 1 - m(O) \end{cases} \tag{5}$$

- If $d > OP1 + \varepsilon$, it means that the grid has exceeded the occupied area of sonar measurement.

Since the grid size is 80*80 in centimeters, it is not sure whether the grid is partially or not in the occupied area of sonar measurement. There are three situations which need to be treated differently: $d\text{-}50 < OP1 - \varepsilon$, $OP1 - \varepsilon < d\text{-}50 < OP1 + \varepsilon$, and $d\text{-}50 > OP1 + \varepsilon$. For the first two situations, the grid is partially in the occupied area of sonar measurement. For the last situation, the grid is not in the occupied area of sonar measurement.

For the first situation $d\text{-}50 < OP1 - \varepsilon$, the function of gbba is:

$$\begin{cases} m(O) = 1 \\ m(E) = 0 \\ m(E \cup O) = 0 \end{cases} \tag{6}$$

For the situation $OP1 - \varepsilon < d\text{-}50 < OP1 + \varepsilon$, there is:

$$\begin{cases} m(O) = 1 - ((d\text{-}25\text{-}(OP1 - \varepsilon))/\varepsilon)^2 \\ m(E) = 0 \\ m(E \cup O) = 1 - m(O) \end{cases} \tag{7}$$

And for the situation $d\text{-}50 > OP1 + \varepsilon$, there will be:

$$\begin{cases} m(O) = 0 \\ m(E) = 0 \\ m(E \cup O) = 1 \end{cases} \tag{8}$$

3.3 Fusion method with DSmT

According to the aforementioned function of gbba discribled, the belief values of the grid states around robot will be calculated in each time slice. In order to achieve effective recognition of grid state, the belief values from different time slice are fused by DSmT theory. For DSmT theory, the combination of more than two evidences can be calculated recursively by the combination of pairwise evidences, which is shown in Fig.3.

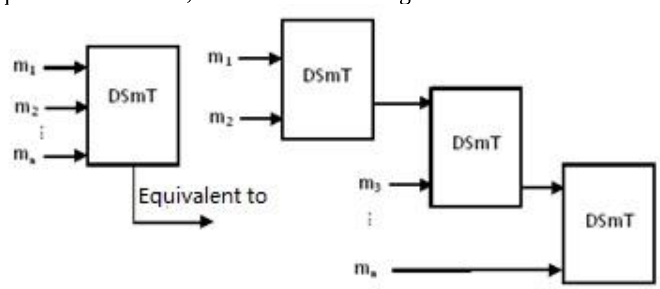

Figure 3 Combination of evidences with DSmT

$m_1, m_2, \ldots, m_n$ respectively denote the state belief value of the same grid at $t_1, t_2, \ldots, t_n$ time slice. On the basis of DSmH rule of combination, the fusion of the grid state belief of current moment(t) and results of the previous moment(t-1) can be made in the following:

$$m_{ij}(\Omega)(C) = \varnothing(C)\left[S_1(C) + S_2(C) + S_3(C)\right] \tag{9}$$

where $m_{ij}()$ stands for the fusion results of line i and column j grid and $C \in D^{\Omega}$. $\varnothing(C)$ is the nonempty characteristic function. For equation (9), there is a constraint: $E \cap O = \Phi$.

According to equation (3), the specific calculation process is as follows:

- If $C=\Phi$, then $m_{ij}(\Phi)=0$.
- If $C=O$, then $\varnothing(O)=1$. There will be: $m_{ij}(O)=S_1(O)+S_2(O)+S_3(O)$. $S_1(O)$, $S_2(O)$, $S_3(O)$ can be respectively calculated as follows:

$$\begin{cases} S_1(O)=m_{ij}^{t-1}(O)\times m_{ij}^{t}(O)+m_{ij}^{t-1}(O)\times m_{ij}^{t-1}(O\cup E) \\ \qquad +m_{ij}^{t-1}(O\cup E)\times m_{ij}^{t}(O) \\ \qquad S_2(O)=0,\ S_3(O)=0 \end{cases} \tag{10}$$

- If $C=E$, then $\varnothing(E)=1$. There is $m_{ij}(E)=S_1(E)+S_2(E)+S_3(E)$, where $S_1(O)$, $S_2(O)$, $S_3(O)$ will respectively be as follows:

$$\begin{cases} S_1(E)=m_{ij}^{t-1}(E)\times m_{ij}^{t}(E)+m_{ij}^{t-1}(E)\times m_{ij}^{t-1}(O\cup E) \\ \qquad +m_{ij}^{t-1}(O\cup E)\times m_{ij}^{t}(E) \\ \qquad S_2(E)=0,\ S_3(E)=0 \end{cases} \tag{11}$$

- If $C=E\cup O$, then $\varnothing(E\cup O)=1$. There will be: $m_{ij}(E\cup O)=S_1(E\cup O)+S_2(E\cup O)+S_3(E\cup O)$, where $S_1(O)$, $S_2(O)$, $S_3(O)$ can be respectively calculated as follows:

$$\begin{cases} S_1(E\cup O)=m_{ij}^{t-1}(E\cup O)\times m_{ij}^{t}(E\cup O) \\ \qquad S_2(E)=0 \\ S_3(E\cup O)=m_{ij}^{t-1}(E)\times m_{ij}^{t}(O)+m_{ij}^{t-1}(O)\times m_{ij}^{t}(E) \end{cases} \tag{12}$$

In the process of calculating the belief value of four states mentioned above, $m_{ij}^{t-1}()$ stands for the fusion result of the grid state belief at moment t-1. And $m_{ij}^{t}()$ represents the grid state belief based on sonar data at moment t.

4 Simulation and Experiments

A simulation software platform for experiments is developed with Microsoft Visual Studio 2013. Reference to Pioneer 2 mobile robot, the simulation software generates the measurement data of 16 sonar sensors(8 in front and 8 in back of robot). The angle settings of eight sonar sensors in front of robot are shown in Fig.4. The coordinate system (Xt Ot Zt) is belonging to mobile robot. The settings of sonar sensors in back of robot are analogous to the setting of sonars in front of the robot.

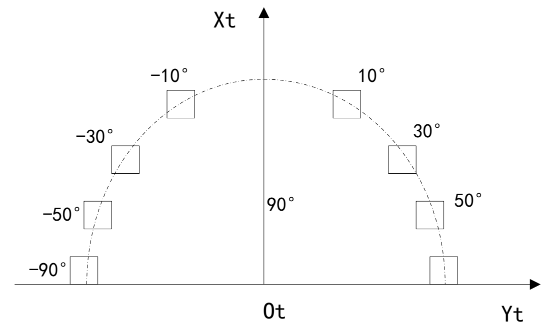

Figure 4 Angle setting of sonar in the front of mobile robot

In the following experiments, the start position of mobile robot is set by user in the simulation software. The end position is always at the upper right corner of the scenario. And the initial angle offset of robot is 0^0.

Fig.5 and 6 are screenshots of the results of two scenarios, where XOY is the world coordinate system and the coordinate axis unit is centimeter. Each grid represents the space of 80*80 cm. The broken lines in Fig.5 and 6 are the traveling routes of the mobile robot. And the start point of the broken line is the start position of the robot.

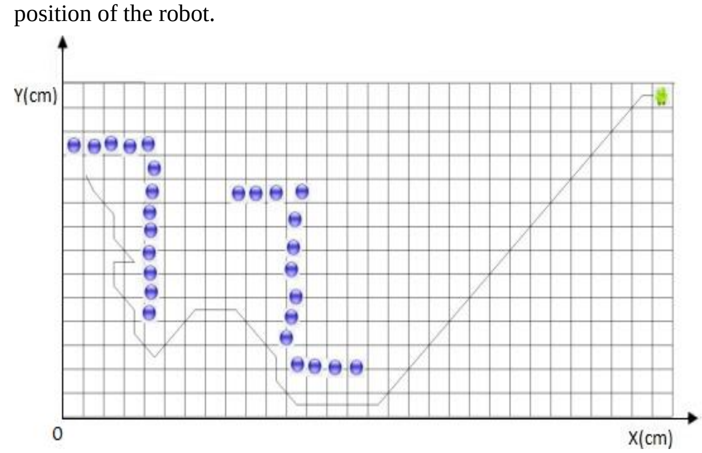

Figure 5 Result of test1

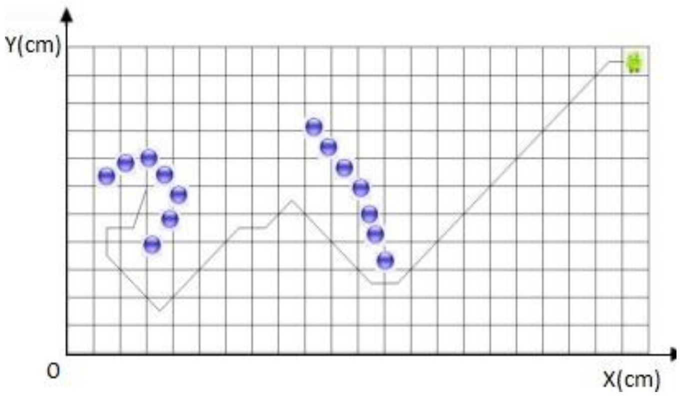

Figure 6 Result of test2

The scenario in Fig.5 includes: a wall with a right angle and a Z-shaped wall. The scenario in Fig.6 includes: a shallow U-shaped trap which depth is about three grids and a straight wall. In both scenarios, robot can avoid obstacles to reach the end point successfully.

In order to test the availability of the method of obstacle avoidance with DSmT, other typical scenarios are provided. And the results of experiments are shown in Table.1.

Table 1. Experiment results of several scenarios

Scenario	runtime/ms	Scenario characteristics
1	640	Wall with a right angle：2(number)
2	375	A wall with two right angle
3	328	A straingt wall
4	453	A wall with a certain curved shape
5	328	A straight wall; A wall with a right angle; (they are adjacent to each other)
6	313	A straight wall; A wall with an angle of about 45 degree; (they are adjacent to each other)
7	688	A wall with a right angle; A Z-shaped wall
8	359	A shallow U-shaped trap
9	469	A shallow U-shaped trap
10	failure	A deep U-shaped trap
11	454	A shallow U-shaped trap; A straight wall

In Table.1, the scenario 7 and 8 are respectively shown in Fig 5 and 6. Since the scenarios in Tab.1 are formed by arranging obstacle targets, the experiment for the scenario with scattered obstacle targetshe is not needed to be done. All the experiments are successful except scenario 10 in Tab.1. Experiments show that the method in the paper is available for the typical scenarios such as straight wall, wall with turning angle and shallow U-shaped trap.

5 Conclusion

The method of Obstacle avoidance by DSmT theory is provided in the paper and the simulation experiments results show that the method is availabe and effective. However, there exits experiment which is failure. It means the method has some drawback. As for future work, we plan to combine with other methods, for example, Bayesian networks, so that it can be successful to avoid obstacles in the scenario with deep U-shaped trap.

ACKNOWLEDGMENTS

The research is supported by Key Science and Technology Program of Shaanxi Province, China (No. 2016GY-112).

REFERENCES

[1] FNM Surname (2018). Article Title. Journal Title, 10(3), 1–10.
[1] YU Zhen-zhong, YAN Ji-hong, et al. Mobile robot path planning based on improved artificial potential field method[J]. Journal of Harbin Institute of Technology, 2011,43(1):50-55.
[2] Wang Fang, Wan Lei, et al. Path planning based on improved artificial potential field for autonomous underwater vehicles[J]. J. Huazhong Univ. Of Sci. & Tech.(Natural Science Edition), 2011, 39(S2): 184-185.
[3] Hacene N, Mendil B. Toward safety navigation in cluttered dynamic environment: A robot neural-based hybrid autonomous navigation and obstacle avoidance with moving target tracking [C]. The 3th International Conference on Control, Engineering and Information Technology. Piscataway, USA: IEEE, 2015: 6pp.
[4] NI Tian, WEI Ruixuan,et al. Neural Dynamic Collision-Avoidance Strategy for Robots Based on Evaluation of Threat Degree[J]. Robot, 2017, 39(6): 853-859.
[5] Wu Chengdong, Zhang Ying, Li Mengxin, et al. A rough set GA-based hybrid method for robot path planning[J]. International Journal of Automation and Computing, 2006, 3(1): 29-34.
[6] LI Zhihai, FU Yili. Motion Planning of a Bio-inspired Biped Wall Climbing Robot Stepping over Obstacles Based on Genetic Algorithm[J]. Robot, 2012,34(6): 751-756.
[7] Dezert J. Foundations for a new theory of plausible and paradoxical reasoning. Inform&Secur.J., Semerdjiev Ed., Bulg. Acad. Of Scl., Vol. 9,2002.
[8] L. Zadeh, A simple view of the Dempster-Shafer theory of evidence and its implication for the rule of combination[J]. AI Magazine 7 (1986): 85–90.
[9] Dezert J. Foundations for a new theory of plausible and paradoxical reasoning[J]. Information and Security Journal, 2002,12(1): 26~30.

[10] Smarandache F, Dezert J. An introduction to DSm theory of plausible, paradoxist, uncertain, and imprecise reasoning for information fusion[J]. Octogon Mathenatical Magazine, 2007, 15(2): 681~722.
[11] Xinhan Huang, Peng Li, et al. Evidence Reasoning Machine Based on DSmT for Mobile Robot Mapping in Unknown Dynamic Environment[C]. Proceedings of the 2009 IEEE International Conference on Robotics and Biomimetics, Guilin, China: 2009 : 753-758.
[12] LI Ji-Gong1, ZHOU Jie-Yong1, et al. Odor sources mapping with D-S inference in time variant airflow environments via a mobile robot. The 5th Annual IEEE International Conference on Cyber Technology in Automation, Control and Intelligent Systems, Shenyang, China: 2015: 545-550.